Transcriptomic Profile of Arabidopsis Rosette Leaves during the Reproductive Stage after Exposure to Ionizing Radiation

Authors: Kim, Jin-Hong, Moon, Yu Ran, Kim, Jae-Sung, Oh, Min-Hyuk, Lee, Ju-Woon, et al.

Source: Radiation Research, 168(3) : 267-280

Published By: Radiation Research Society

URL: https://doi.org/10.1667/RR0963.1

RADIATION RESEARCH **168**, 267–280 (2007)
0033-7587/07 $15.00

Transcriptomic Profile of *Arabidopsis* Rosette Leaves during the Reproductive Stage after Exposure to Ionizing Radiation

Jin-Hong Kim,[a] Yu Ran Moon,[a] Jae-Sung Kim,[a] Min-Hyuk Oh,[b] Ju-Woon Lee[a] and Byung Yeoup Chung[a,1]

[a] *Advanced Radiation Research Institute (ARTI), Korea Atomic Energy Research Institute (KAERI), 1266 Shinjeong-dong, Jeongeup-si, Jeollabuk-do 580-185, Korea; and* [b] *Department of Molecular Biology, Pusan National University, Busan 609-735, Korea*

Kim, J-H., Moon, Y. R., Kim, J-S., Oh, M-H., Lee, J-W. and Chung, B. Y. Transcriptomic Profile of *Arabidopsis* Rosette Leaves during the Reproductive Stage after Exposure to Ionizing Radiation. *Radiat. Res.* 168, 267–280 (2007).

We attempted to obtain a transcriptomic profile of ionizing radiation-responsive genes in *Arabidopsis* plants using Affymetrix ATH1 whole-genome microarrays. The *Arabidopsis* plants were irradiated with 200 Gy γ rays at the early reproduction stage, 33 days after sowing. Rosette leaves were harvested during the postirradiation period from 36 to 49 days after sowing and used for the microarray analysis. The most remarkable changes in the genome-wide expression were observed at 42 days after sowing (9 days after the irradiation). We identified 2165 genes as γ-ray inducible and 1735 genes as γ-ray repressible. These numbers of affected genes were almost two to seven times higher than those at other times. In a comparison of the control and irradiated groups, we also identified 354 differentially expressed genes as significant by applying Welch's *t* test and fold change analysis. The gene ontology analysis showed that radiation up-regulated defense/stress responses but down-regulated rhythm/growth responses. Specific expression patterns of 10 genes for antioxidant enzymes, photosynthesis or chlorophyll synthesis after irradiation were also obtained using real-time quantitative PCR analysis. We discuss physiological and genetic alterations in the antioxidative defense system, photosynthesis and chlorophyll metabolism after irradiation at the reproductive stage.

INTRODUCTION

The development of techniques for genetic evaluation of biochemical and physiological responses of plant cells to environmental stress factors has allowed enormous advances in our understanding of stress-inducible signaling mechanisms as well as offering promising genetic targets to generate transgenic plants that can tolerate multiple stresses (*1–3*). However, few advances have been reported for plant research in the field of radiation biology because of both experimental limitations and political/social restrictions. The lack of large-capacity facilities for irradiation and/or low-dose radiation fields (or greenhouses) for long-term research makes plants unattractive for radiation biology studies. Therefore, it has been unusual for ionizing radiation to be used as a mutagen to broaden the genetic spectrum of major crop plants (*4*). The mechanism of action by which radiation induces genetic alterations in cells has been elucidated by studies using *in vitro* systems (*5–8*). A recent report on radiation-induced DNA damages inducing mutations reinforced the concept that the sensitivity of genes to radiation depends on the base composition and/or the spatial localization of the gene on the chromosome (*8*). The scientific bases of this theory are universal enough to be applicable to both plant and animal systems. Genome-wide transcript profiling was performed using human cell lines exposed to radiation to elucidate changes in intracellular signaling (*9*). In that study, 19 genes were identified to be differentially expressed in cell cycle regulation, three in apoptosis, and four in nucleotide excision repair. This information increases our understanding of radiation responses at the gene expression level. In spite of some functional similarities of genes in plant and animal systems, however, differences in the genetic backgrounds have limited the use of expression profiles to identify cell signaling in both plants and animals (*10*). Accordingly, the need for genome-wide analyses of plant transcripts is increasing in the field of radiation biology. Transcriptional and post-transcriptional regulation to determine radiation-mediated signaling in plant cells has rarely been investigated on a genome-wide scale. In contrast, the physiological/ecological responses in irradiated plants have been investigated extensively (*11–15*).

It has generally been presumed that radiation-induced damages to DNA occur through both direct energy deposition into the sugar-phosphate moiety and interactions with reactive oxygen species (ROS), generally hydroxyl radical (OH) produced by water radiolysis (*8, 16, 17*). In addition, cellular responses to radiation can occur through direct participation of ROS in cell signaling (*18, 19*) and/or indirect involvement of low-molecular-weight signaling factors released from the reactions of ROS and neighboring cellular

[1] Address for correspondence: Advanced Radiation Research Institute, Korea Atomic Energy Research Institute, 1266 Shinjeong-dong, Jeongeup-si, Jeollabuk-do 580-185, Korea, e-mail: bychung@kaeri.re.kr.

TABLE 1
Primer Sequences Used in Quantitative RT-PCR Experiment

Locus name	Gene name	Forward/reverse primer
At1g49240	*actin2*	5′GCCCAGAAGTCTTGTTCCAG3′/ 5′CTTGGTGCAAGTGCTGTGAT3′
At1g58290	*hemAl*	5′AGGAAAGCAATGGAAGCTCA3′/ 5′AAGTCATCAACCGCTCTCGT3′
At4g27440	*porB*	5′CACTTTCGCTTCGCTTTACC3′/ 5′CAGCTCCAATAAACCCCTGA3′
At2g40100	*Ihcb4.3*	5′AAAACCTTGCCAAGAACGTG3′/ 5′TTGCCATGCAATTCCTGTAA3′
At1g08830	*csd1*	5′ACATTTCAACCCCGATGGTA3′/ 5′GAGGTCATCAGGGTCTGCAT3′
At2g28190	*csd2*	5′AAGAAGGCTGTTGCAGTGCT3′/ 5′AGGGTTGAAATGTGGTCCTG3′
At4g25100	*fsd1*	5′TCACTGGGGAAAACATCACA3′/ 5′CTCCACCACCTGGTTTCATT3′
At4g08390	*sapx*	5′GGTCCTGAGGATTGTCCAGA3′/ 5′CTCCAGGTCCTTCTTTCGTG3′
At4g35090	*cat2*	5′TTCAAACCCGTGTCTTCTCC3′/ 5′TTCTCAGCATGACGAACCTG3′
At1g 19570	*dhar*	5′TCCAATGACGGATCTGAACA3′/ 5′TATGGACATGGGGAAAGCTC3′
At4g31870	*gp*	5′TCAAACCCTGAGATCAAGCA3′/ 5′TCTCGACAACTTTGCCCTTT3′

components (*20, 21*). Therefore, ROS are critical mediators of intracellular signaling of radiation responses, and ROS-scavenging (antioxidant) enzyme activities are also crucial factors in propagation of radiation responses. Accordingly, studies on the physiology of stress using radiation may provide information about its ability to confer tolerance to multiple stresses to plants (*11, 13, 15*). Such studies may help improve the survival of plants under deteriorating environmental conditions, e.g., frequent droughts and floods, and increased exposure to UV radiation and may have applications in the detection and evaluation of radioactive materials near nuclear accident sites (*15, 22*). Profiling of radiation-induced/repressed transcripts can be used to increase the efficiencies of mutation and screening for desirable phenotypes in plants. To date, genome-wide changes in the expressions of genes in *Arabidopsis* have been documented after treatments with auxin and brassinosteroid (*1*), chitin (*23*), hypoxia (*24*), and oxidative stress-causing agents such as methyl viologen, *Alternaria alternata* toxin, 3-aminotriazole and ozone (*2*). Profiling of candidate genes involved in cell cycle regulation (*25, 26*) or wax biosynthesis (*27*) has been also reported using *Arabidopsis* microarrays. *Arabidopsis* is an attractive plant model for radiation biology because of its short generation time, genetic simplicity, and availability of whole genome information. Recently, the responses of hundreds of plant genes to radiation were characterized through a short-term global transcription analysis in *Arabidopsis*, and *cis*-acting elements in the promoter regions of the radiation-responsive genes were also analyzed (*28–35*). Most altered genes were involved in cell growth, cell division, development, translation, general metabolism, signal transduction, and stress/defense response. However, a long-term genome-scale profiling of transcripts responding to radiation in plants at the reproductive stage has not been reported for any plant species, including *Arabidopsis*.

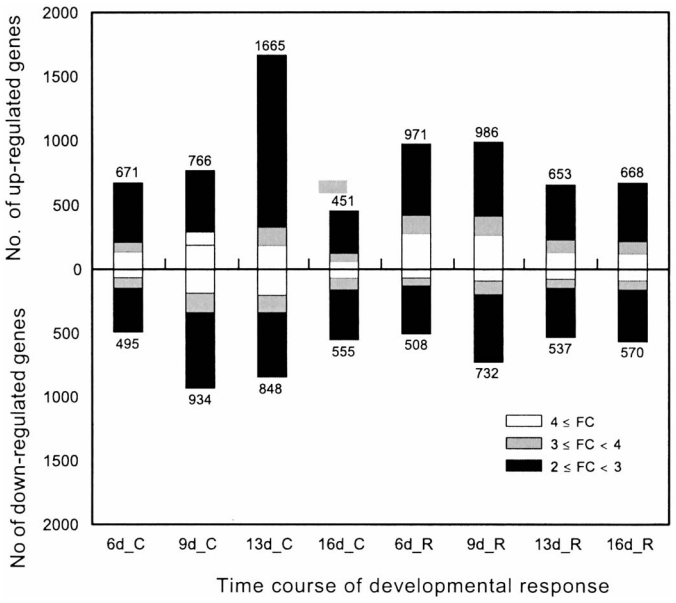

FIG. 1. Transcript level changes in leaves during the reproduction stage. The numbers of genes with a two-, three-, or fourfold increase or decrease in expression in the 6-, 9-, 13- or 16-day plants compared to the 3-day plants after γ irradiation are represented by black, gray and white bars, respectively. Data were analyzed as described in the Materials and Methods. FC, fold change; C, control; R, γ-irradiated.

Massive doses of radiation have been shown to induce physical changes in plants, including enhancement of respiration, increase in ethylene production, induction of en-

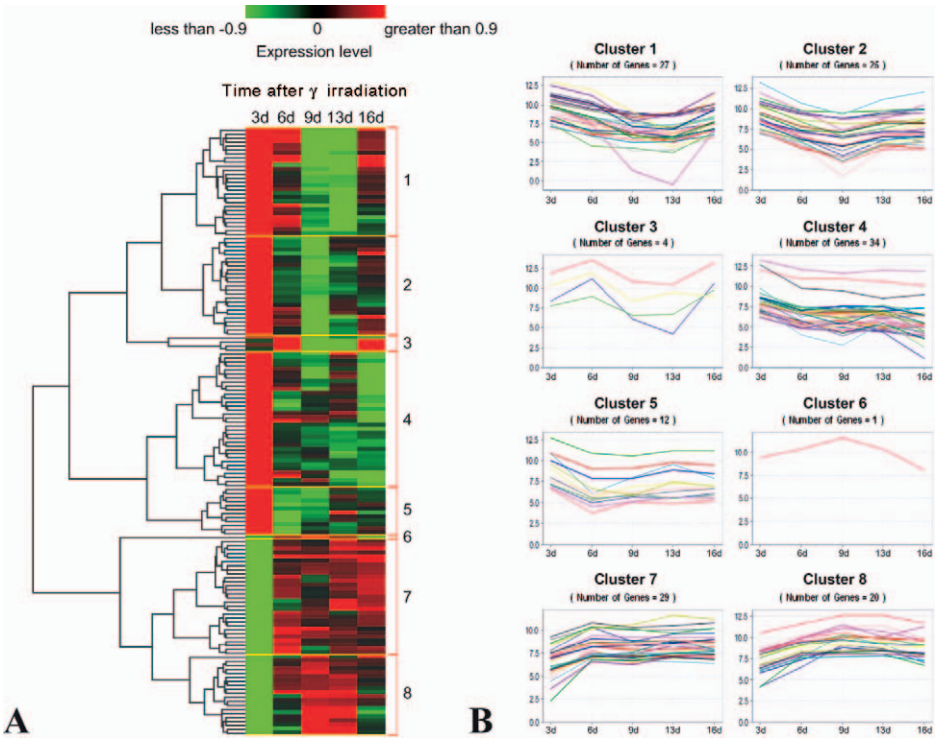

FIG. 2. Clustering analysis of gene expression in control leaves during the reproduction stage. Panel A: Hierarchical cluster analysis. Each horizontal line shows the expression data for one gene after normalization at the times indicated. Colors show the normalized expression level. Induction (or repression) ranges from black to red (or green) with a fold-change scale bar shown above the cluster. Numbers (1 to 8) indicate defined sub-branches or clusters. Panel B: The eight hypothetical profiles are displayed as Clusters 1 to 8 with the number of genes found in each cluster. Each line represents the expression of one gene.

zyme activities, and accumulation of sucrose and specific protein species (*12*). Photosynthesis and antioxidative defense systems have long been studied in relation to the radiation responses of various plant species (*11, 13, 15, 30*). These sensitive systems continue to be interesting subjects in plant radiation biology. However, the stress sensitivity of a plant can differ depending on the developmental stage (*36, 37*), and this is not limited to radiation. We first determined the developmental stage of *Arabidopsis* showing the most dramatic alterations in the phenotypic traits after exposure to γ rays at a dose of 200 Gy, which induced noticeable phenotypic changes in *Arabidopsis* seedlings in a preliminary experiment. Interestingly, the early reproduction stage within 4–5 weeks after seeds were sown was the most sensitive to radiation, with the irradiated plants showing inhibition of stem growth, retardation of leaf senescence, accumulation of chlorophyll and carotenoid, and elevation of photosynthetic saturation for light use. To gain more insight into how plants respond to radiation at the genome level, we carried out gene expression profiling using *Arabidopsis* leaves sampled at five times: 3, 6, 9, 13 and 16 days after the plants were irradiated with 200 Gy γ rays at the early reproduction stage. Affymetrix ATH1 oligonucleotide GeneChip arrays were used to cover the whole genome representing nearly all the nuclear, plastid and mitochondrial genes encoded in *Arabidopsis*. The goal was to generate an informative transcriptomic profile of plant genes responding to radiation at the reproductive stage through a long-term genome-scale analysis of *Arabidopsis* genes. The results allowed for the genome-wide identification of genes with significant positive or negative changes in expression (induced and repressed, respectively) in response to radiation in plants at the reproductive stage. This paper presents characteristics of radiation responses during the reproduction stage, identifying the radiation-responsive genes related to photosynthesis and antioxidant enzymes.

MATERIALS AND METHODS

Plant Materials and γ Irradiation

Arabidopsis thaliana ecotype Columbia (Col-0) was used in this study. Seedlings were grown for 33 days after sowing at 22/18°C (day/night) with a 16-h photoperiod in a compound soil mixture (vermiculite:peat moss:perlite = 1:1:1). They were exposed to 200 Gy γ rays (dose rate 50 Gy/h) generated by a ^{60}Co γ irradiator (150 TBq of capacity; AECL, Canada) at the Korea Atomic Energy Research Institute. The irradiated seedlings were placed under the same growth conditions as described above. Then their rosette leaves were detached and immediately frozen in liquid nitrogen at 3, 6, 9, 13 and 16 days after irradiation, which corresponded to 36, 39, 42, 46 and 49 days after sowing, respectively. The leaves were stored at −80°C until RNA isolation.

RNA Preparation and Microarray Analysis

To minimize interplant variability, rosette leaves from a minimum of 10 plants were pooled for each RNA extraction. Total RNA was extracted

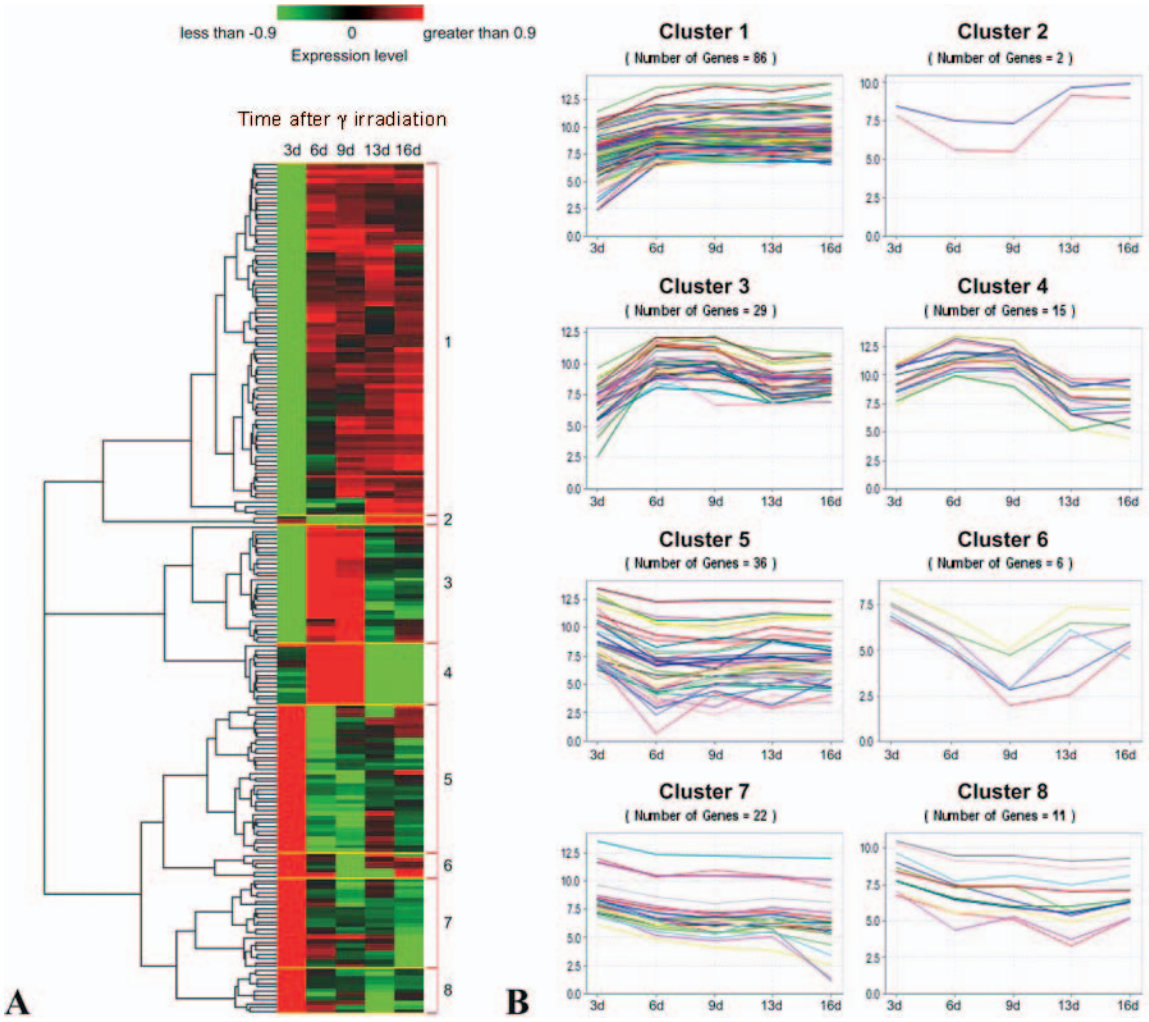

FIG. 3. Clustering analysis of gene expression in the irradiated leaves during the reproduction stage. Panel A: Hierarchical cluster analysis. Each horizontal line shows the expression data for one gene after normalization at the times indicated. Colors show the normalized expression level. Induction (or repression) ranges from black to red (or green) with a fold-change scale bar shown above the cluster. Numbers (1 to 8) indicate defined subbranches or clusters. Panel B: The eight hypothetical profiles are displayed as Clusters 1 to 8 with the number of genes found in each cluster. Each line represents the expression of one gene.

from the leaves using Trizol (Invitrogen, Carlsbad, CA) and further purified using an RNeasy Mini Kit (Qiagen, Valencia, CA) following the manufacturer's specifications. The amount of RNA was determined by spectrophotometry at 260 nm, and its integrity was assessed by analyzing the ribosomal RNA bands after gel electrophoresis. Conversion of total RNA into double-stranded cDNA, generation of biotin-labeled cRNA from the double-stranded cDNA, and hybridization of the biotin-labeled cRNA with the GeneChip® Arabidopsis ATH1 Genome Array (Affymetrix, Santa Clara, CA) were performed and analyzed as recommended by Affymetrix.

Data Analysis

GenPlex™ v1.8 software (ISTECH Inc., Goyang city, South Korea) was used for data analysis. The MAS5 algorithm was used for expression summary and signal calculation. Global scaling normalization using a GCOS algorithm was performed, and then the normalized data were $\log_2$-transformed. Fold change and Welch's *t* test were applied to select the differentially expressed genes. The difference was more than twofold, and the significance level was 0.05. To better visualize and compare the two methods for differentially expressed genes, a volcano plot was used. The twofold differentially expressed genes were clustered using hierarchical clustering with Pearson correlation as a similarity measure and complete linkage as a linkage method (*38–40*). The top 200 differentially expressed genes with the greatest fold change were classified into functional subgroups by BINGO, which enables Gene Ontology significance analysis (*41*). Pathway analysis was performed using the Kyoto Encyclopedia of Genes and Genomes (KEGG) pathway database, which is available online (http://www.genome.jp/kegg/pathway.html).

Real-Time Quantitative PCR Analysis

One microgram of total RNA was reverse-transcribed into cDNA using AccuPower RT Premix (Bioneer, Daejeon, Korea) for 60 min at 42°C using 0.5 μg anchored oligo(dT)$_{18}$V primers. Real-time PCR was carried out in a 25-μl reaction mixture containing 1 μl template cDNA, 12.5 μl SYBR®Premix Ex Taq™ (2×) (Takara Bio Inc., Otsu, Japan), 2 μl forward primer (10 μ*M*), 2 μl reverse primer (10 μ*M*), and 7.5 μl distilled water, using a Smart Cycler® II System (Cepheid, Sunnyvale, CA). Gene-specific primer sets used are listed in Table 1. The thermal profile consisted of 1 cycle at 95°C for 1 min followed by 45 cycles at 95°C for 5 s, 56°C for 20 s, and 72°C for 15 s. For each run, data acquisition and analysis were done using the Smart Cycler® software (version 2.0b, Cepheid. Then the relative transcript level was determined using the com-

TABLE 2
Gene Ontology Analysis of Differentially Expressed Genes in Control (A) and Irradiated (B) Samples during the Reproduction Stage

Days after irradiation	GOC	GO_ID	GO term	C	*P* value	k
A: Control						
	Up-regulation					
6	BP	GO:0009628	response to abiotic stimulus	224/16475 (1.4)	0.0168	7/150 (4.7)
	CC	GO:0005623	cell	11389/16475 (69.1)	0.1123	112/150 (74.6)
	MF	GO:0016462	pyrophosphatase activity	235/16475 (1.4)	0.0058	8/150 (5.3)
9	BP	GO:0009605	response to external stimulus	366/16475 (2.2)	0.0002	13/158 (8.2)
	CC	GO:0005576	extracellular region	61/16475 (0.4)	0.1161	3/158 (1.9)
	MF	GO:0008194	UDP-glycosyltransferase activity	109/16475 (0.7)	0.0006	7/158 (4.4)
13	BP	GO:0006950	response to stress	376/16475 (2.3)	0.0006	12/147 (8.2)
	CC	GO:0012505	endomembrane system	3426/16475 (20.8)	0.0372	41/147 (27.9)
	MF	GO:0005386	carrier activity	336/16475 (2.0)	0.0032	10/147 (6.8)
16	BP	GO:0006519	amino acid and derivative metabolism	254/16475 (1.5)	0.0014	9/139 (6.4)
	CC	GO:0043231	intracellular membrane-bound organelle	6455/16475 (39.2)	0.1893	61/139 (43.9)
	MF	GO:0004066	asparagine synthase activity	2/16475 (0.0)	0.0168	2/139 (1.4)
	Down-regulation					
6	BP	GO:0009719	response to endogenous stimulus	369/16475 (2.2)	0.0001	13/147 (8.8)
	CC	GO:0016020	membrane	4667/16475 (28.3)	0.0039	58/147 (39.5)
	MF	GO:0003700	transcription factor activity	1342/16475 (8.1)	0.0018	24/147 (16.3)
9	BP	GO:0042545	cell wall modification	40/16475 (0.2)	0.0000	8/156 (5.1)
	CC	GO:0016020	membrane	4667/16475 (28.3)	0.0000	81/156 (51.9)
	MF	GO:0016799	hydrolase activity	13/16475 (0.1)	0.0002	4/156 (2.6)
13	BP	GO:0009828	cell wall loosening	32/16475 (0.2)	0.0000	7/164 (4.3)
	CC	GO:0016020	membrane	4667/16475 (28.3)	0.0000	94/164 (57.3)
	MF	GO:0016798	hydrolase activity	150/16475 (0.9)	0.0001	9/164 (5.5)
16	BP	GO:0007275	development	382/16475 (2.3)	0.0006	12/147 (8.2)
	CC	GO:0016020	membrane	4667/16475 (28.3)	0.0000	66/147 (44.9)
	MF	GO:0015290	transporter activity	195/16475 (1.2)	0.0018	8/147 (5.4)
B: Irradiated						
	Up-regulation					
6	BP	GO:0006952	defense response	315/16475 (1.9)	0.0000	13/155 (8.4)
	CC	GO:0031225	anchored to membrane	219/16475 (1.3)	0.0011	9/155 (5.8)
	MF	GO:0030528	transcription regulator activity	1450/16475 (8.8)	0.0022	26/155 (16.8)
9	BP	GO:0006952	defense response	315/16475 (1.9)	0.0000	15/159 (9.4)
	CC	GO:0012505	endomembrane system	3426/16475 (20.8)	0.0018	50/159 (31.4)
	MF	GO:0030528	transcription regulator activity	1450/16475 (8.8)	0.0015	27/159 (17.0)
13	BP	GO:0006952	defense response	315/16475 (1.9)	0.0000	18/143 (12.6)
	CC	GO:0012505	endomembrane system	3426/16475 (20.8)	0.0002	49/143 (34.3)
	MF	GO:0016740	transferase activity	1908/16475 (11.6)	0.0036	29/143 (20.3)
16	BP	GO:0009607	response to biotic stimulus	399/16475 (2.4)	0.0000	20/154 (13.0)
	CC	GO:0016602	CCAAT-binding factor complex	11/16475 (0.1)	0.0001	4/154 (2.6)
	MF	GO:0009055	electron carrier activity	49/16475 (0.3)	0.0011	5/154 (3.2)
	Down-regulation					
6	BP	GO:0048511	rhythmic process	17/16475 (0.1)	0.0004	4/142 (2.8)
	CC	GO:0005634	nucleus	697/16475 (4.2)	0.3949	8/142 (5.6)
	MF	GO:0030528	transcription regulator activity	1450/16475 (8.8)	0.0001	28/142 (19.7)
9	BP	GO:0007623	circadian rhythm	17/16475 (0.1)	0.0003	4/131 (3.1)
	CC	GO:0031225	anchored to membrane	219/16475 (1.3)	0.5219	3/131 (2.3)
	MF	GO:0030528	transcription regulator activity	1450/16475 (8.8)	0.0051	22/131 (16.8)
13	BP	GO:0009733	response to auxin stimulus	117/16475 (0.7)	0.0005	7/141 (5.0)
	CC	GO:0016020	membrane	4667/16475 (28.3)	0.0001	62/141 (44.0)
	MF	GO:0005372	water transporter activity	28/16475 (0.2)	0.0017	4/141 (2.8)
16	BP	GO:0009733	response to auxin stimulus	117/16475 (0.7)	0.0000	11/148 (7.4)
	CC	GO:0016020	membrane	4667/16475 (28.3)	0.0005	62/148 (41.9)
	MF	GO:0016837	carbon-oxygen lyase activity	26/16475 (0.2)	0.0226	3/148 (2.0)

Notes. Differentially expressed genes were selected to have more than a twofold change in the respective samples relative to the 3-day control. GOC, BP, CC and MF represent the GO category, biological process, cellular component, and molecular function. GO terms in the table were selected for their highest significance based on *P* values in each GO category. C, the total frequency of a given GO term in all annotations in the *Arabidopsis* genome; k, cluster frequency of a given GO term in the differentially expressed genes selected. Numbers in parentheses are percentages.

TABLE 3
Pathway Analysis of the Differentially Expressed Genes during the Reproduction Stage

KEGG pathway	Gene counts
Control	
Stilbene, coumarine and lignin biosynthesis	9
gamma-Hexachlorocyclohexane degradation	8
Ribosome	8
Photosynthesis	8
Limonene and pinene degradation	8
Fluorene degradation	8
Ascorbate and aldarate metabolism	8
Oxidative phosphorylation	5
Phenylalanine metabolism	4
Tyrosine metabolism	3
Irradiated	
Stilbene, coumarine and lignin biosynthesis	11
Ribosome	11
gamma-Hexachlorocyclohexane degradation	9
Limonene and pinene degradation	9
Fluorene degradation	9
Ascorbate and aldarate metabolism	9
Oxidative phosphorylation	5
Purine metabolism	4
Photosynthesis	3
Glutathione metabolism	3

Notes. List includes the top 10 pathways based on gene counts. Differentially expressed genes for the control and irradiated samples relative to the 3-day controls were 3347 and 3220 genes in combination, respectively. The pathway analysis was performed using 57 and 53 genes with pathway information among these, respectively.

parative ($2^{-\Delta\Delta Ct}$) method (*42, 43*). Relative quantification of gene expression using the $2^{-\Delta\Delta Ct}$ method was correlated with the absolute gene quantification obtained using calibration curves (*44*). *Actin2* was used as an endogenous control gene to normalize for differences in the amounts of total RNA.

RESULTS AND DISCUSSION

Despite many recent analyses of radiation-regulated gene expression in various animal cells by cDNA or oligonucleotide microarrays (*9, 45–47*), there are no genome-wide profiles for the long-term expression of genes in plants exposed to radiation. We attempted to analyze radiation-regulated cellular responses at the transcriptional level in *Arabidopsis* plants, specifically leaves, during the reproduction stage.

Gene Expression of the Control and Irradiated Groups during the Reproduction Stage

We first aimed to determine which genes are expressed and/or regulated during the reproduction stage in the control and irradiated plants. Leaves were harvested at 3, 6, 9, 13 and 16 days after irradiation, which corresponded to 36, 39, 42, 46 and 49 days after sowing, respectively. Transcript levels were calculated relative to the respective 3-day samples and differentially expressed genes were selected with a twofold change and a significance level of 0.05 after $\log_2$

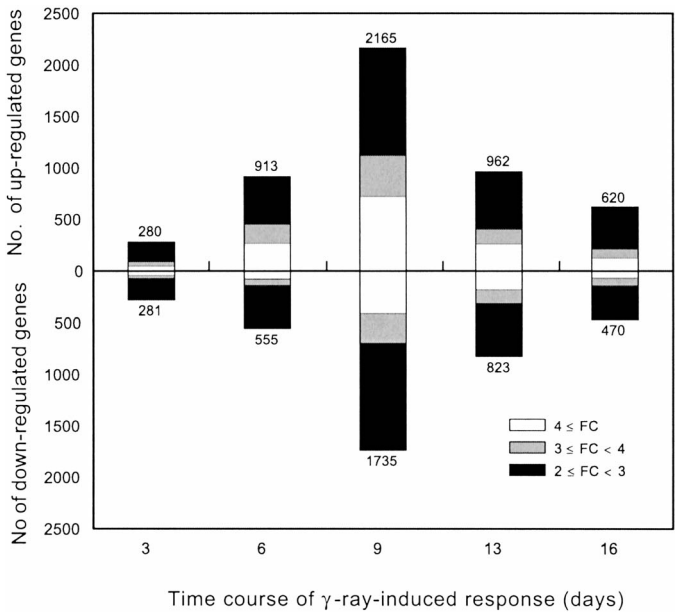

FIG. 4. Transcript level changes in leaves during the postirradiation period. The numbers of genes with a two-, three- or fourfold increase or decrease in expression in the γ-irradiated plants compared to the control plants at different times after γ irradiation are represented by black, gray and white bars, respectively. Data were processed as described in the Materials and Methods. FC, fold change.

transformation of the normalized data. The 3-day samples were used as a control instead of the 0-day samples to exclude the effects of short-term fluctuations in the expression of genes after γ irradiation. Gene expression levels in leaves decrease in terms of the amounts of transcripts during the reproduction stage (*36*). In the present study, however, the total number of genes affected increased in the control leaves up to 13 days after irradiation and then decreased at 16 days after the irradiation, while the irradiated leaves showed the maximum expression change at 9 days after the irradiation (Fig. 1). The proportion of genes showing an increased transcript level was generally higher in the irradiated leaves than in the control leaves except for the 13-day samples.

The numbers of differentially expressed genes in the control and irradiated groups were 3347 and 3220 in combination during the postirradiation period, respectively, while only 152 and 207 differentially expressed genes existed in common throughout that period. These common differentially expressed genes were classified into two or three major groups using hierarchical clustering with Pearson correlation as a similarity measure and complete linkage as a linkage method (Figs. 2A and 3A). This result indicates that 6 days after the irradiation or 39 days after sowing can be a turning point in gene expression during the reproduction stage. Finally, the data set clusters suggest that although the majority of genes are either continuously up-regulated or down-regulated, there are also groups showing alternative patterns of expression (*26*). We identified two groups (Clus-

TABLE 4
Radiation Responsive Genes during the Postirradiation Period

Days after irradiation	Average $\log_2$(FC)	Transcript ID	Gene name
(A)			
	Induced genes		
3	2.4194489	At5g40150	peroxidase, putative
6	2.4055262	At4g33420	peroxidase, putative
	2.0559115	At5g48450	multi-copper oxidase type I family protein
	1.765161	At2g29170	short-chain dehydrogenase/reductase (SDR) family protein
	1.7520266	At3g28200	peroxidase, putative
	1.7306409	At3g50930	AAA-type ATPase family protein
	1.6923962	At2g37540	short-chain dehydrogenase/reductase (SDR) family protein
	1.3828316	At1g23020	ferric-chelate reductase, putative
	1.3707452	At5g64120	peroxidase, putative
9	3.43536	At2g28190	superoxide dismutase (Cu-Zn), chloroplast (SODCP) (CSD2)
	2.7038298	At1g12520	superoxide dismutase copper chaperone, putative
	2.4422855	At3g28200	peroxidase, putative
	2.279912	At5g40150	peroxidase, putative
	2.144084	At4g09010	L-ascorbate peroxidase, chloroplast, putative
	2.0108862	At5g64120	peroxidase, putative
	1.9585624	At5g51100	superoxide dismutase (Fe), putative
	1.8616467	At1g71695	peroxidase 12 (PERI2) (PI2) (PRXR6)
	1.6058083	At1g08830	superoxide dismutase (Cu-Zn) (SODCC) (CSD1)
	1.5956535	At5g23310	superoxide dismutase (Fe) (FSD3)
	1.5212107	At1g77490	L-ascorbate peroxidase, thylakoid-bound (tAPX)
	1.4836998	At5g51890	peroxidase-related
	1.383935	At4g33420	peroxidase, putative
13	3.369529	At5g51890	peroxidase-related
	2.350175	At1g71695	peroxidase 12 (PERI2) (PI2) (PRXR6)
	1.8598824	At2g28190	superoxide dismutase (Cu-Zn), chloroplast (SODCP) (CSD2)
	1.7416306	At4g03060	2-oxoglutarate-dependent dioxygenase, putative (AOP2)
	1.6883192	At1g19570	dehydroascorbate reductase, putative
	1.5280867	At4g08390	L-ascorbate peroxidase, stromal (sAPX)
	1.3948259	At4g09010	L-ascorbate peroxidase, chloroplast, putative
	1.3385196	At2g22420	peroxidase 17 (PERI7) (PI7)
	1.2742739	At4g25100	superoxide dismutase (Fe), chloroplast (SODB) (FSD1)
	1.1855841	At4g10500	oxidoreductase, 2OG-Fe(II) oxygenase family protein
	1.0841036	At1g08830	superoxide dismutase (Cu-Zn) (SODCC) (CSD1)
16	3.0575595	At4g08390	L-ascorbate peroxidase, stromal (sAPX)
	2.2580771	At1g28030	oxidoreductase, 2OG-Fe(II) oxygenase family protein
	2.2224302	At4g25100	superoxide dismutase (Fe), chloroplast (SODB) (FSD1)
	1.3870687	At4g36430	peroxidase, putative
	1.3563209	At2g29350	tropinone reductase, putative
	1.3140545	At1g19570	dehydroascorbate reductase, putative
	Repressed genes		
3	−1.7209291	At4g39830	L-ascorbate oxidase, putative
	−1.3683543	At1g29160	Dof-type zinc finger domain-containing protein
	−1.1702714	At5g19890	peroxidase, putative
	−1.101944	At1g17020	oxidoreductase, 2OG-Fe(II) oxygenase family protein
6	−2.2576113	At1g17020	oxidoreductase, 2OG-Fe(II) oxygenase family protein
	−1.4576573	At3g42570	peroxidase, putative
	−1.3152676	At4g08390	L-ascorbate peroxidase, stromal (sAPX)
	−1.2995005	At4g03060	2-oxoglutarate-dependent dioxygenase, putative (AOP2)
	−1.1865816	At4g25100	superoxide dismutase (Fe), chloroplast (SODB) (FSD1)
	−1.1730733	At4g25300	oxidoreductase, 2OG-Fe(II) oxygenase family protein
	−1.1638432	At4g32320	peroxidase family protein
	−1.039835	At1g06620	2-oxoglutarate-dependent dioxygenase, putative
	−1.0072231	At1g07890	L-ascorbate peroxidase 1, cytosolic (APX1)
9	−2.6704993	At4g10500	oxidoreductase, 2OG-Fe(II) oxygenase family protein
	−2.6589546	At3g42570	peroxidase-related
	−2.4284115	At4g25100	superoxide dismutase (Fe), chloroplast (SODB) (FSD1)
	−2.3921642	At1g17020	oxidoreductase, 2OG-Fe(II) oxygenase family protein

(continued on page 274)

TABLE 4
(continued)

Days after irradiation	Average $\log_2$(FC)	Transcript ID	Gene name
	−2.1933298	At2g29370	tropinone reductase, putative
	−1.8451958	At2g29320	tropinone reductase, putative
	−1.651741	At2g29990	pyridine nucleotide-disulphide oxidoreductase family protein
	−1.4436169	At4g31870	glutathione peroxidase, putative
	−1.4195185	At4g32320	peroxidase family protein
	−1.3083835	At4g08390	L-ascorbate peroxidase, stromal (sAPX)
	−1.2154627	At4g35090	catalase 2
	−1.0904951	At3g49120	peroxidase 33 (PER33) (P33) (PRXCA)
13	−2.2513075	At4g31870	glutathione peroxidase, putative
	−2.238213	At2g29370	tropinone reductase, putative
	−1.6643324	At1g17020	oxidoreductase, 2OG-Fe(II) oxygenase family protein
	−1.5291271	At1g23020	ferric-chelate reductase, putative
	−1.5120478	At4g32320	peroxidase family protein
	−1.303483	At4g35090	catalase 2
	−1.2666025	At2g37130	peroxidase 21 (PER21) (P21) (PRXR5)
	−1.2456388	At2g31570	glutathione peroxidase, putative
	−1.0318995	At5g19890	peroxidase, putative
	−1.0165234	At1g29160	Dof-type zinc finger domain-containing protein
	−1.0164618	At4g33870	peroxidase, putative
16	−2.074337	At1g23020	ferric-chelate reductase, putative
	−1.218318	At4g35090	catalase 2
	−1.2676253	At4g33420	peroxidase, putative
	−1.1945162	At2g29300	tropinone reductase, putative
(B)			
	Induced genes		
3	3.1086726	At5g54190	NADPH-protochlorophyllide oxidoreductase A (PORA)
6	2.074326	At5g54190	NADPH-protochlorophyllide oxidoreductase A (PORA)
	1.8820562	At3g27690	chlorophyll A-B binding protein (LHCB2:4)
	1.4740295	At4g27440	NADPH-protochlorophyllide oxidoreductase B (PORB)
9	2.663498	At5g54190	NADPH-protochlorophyllide oxidoreductase A (PORA)
	2.5387745	At3g27690	chlorophyll A-B binding protein (LHCB2:4)
	2.2573128	At1g19150	LHCI type II, putative
	2.0492506	At4g27440	NADPH-protochlorophyllide oxidoreductase B (PORB)
	2.0414686	At5g45930	Mg-protoporphyrin IX chelatase, putative
	1.3696604	At1g03630	NADPH-protochlorophyllide oxidoreductase C (PORC)
	1.3261137	At1g19670	coronatine-induced protein 1 (CORI1)
	1.219584	At1g64590	short-chain dehydrogenase/reductase (SDR) family protein
13	4.059266	At3g27690	chlorophyll A-B binding protein (LHCB2:4)
	2.08077	At1g58290	glutamyl-tRNA reductase 1 (HEMA1)
	1.6156063	At4g27440	NADPH-protochlorophyllide oxidoreductase B (PORB)
	1.4812336	At1g19670	coronatine-induced protein 1 (CORI1)
	1.1018019	At1g19150	LHCI type II, putative
	1.0646944	At1g15820	chlorophyll A-B binding protein (LHCB6)
16	2.4675798	At3g27690	chlorophyll A-B binding protein (LHCB2:4)
	1.7152658	At1g58290	glutamyl-tRNA reductase 1 (HEMA1)
	1.5346851	At4g27440	NADPH-protochlorophyllide oxidoreductase B (PORB)
	Repressed genes		
6	−1.3056841	At2g40100	chlorophyll A-B binding protein (LHCB4.3)
9	−1.8259163	At2g40100	chlorophyll A-B binding protein (LHCB4.3)
	−1.11796	At1g76570	chlorophyll A-B binding family protein
	−1.0365758	At3g14440	9-cis-epoxycarotenoid dioxygenase, putative
13	−1.5352154	At1g76570	chlorophyll A-B binding family protein
	−1.5352154	At2g40100	chlorophyll A-B binding protein (LHCB4.3)
16	−2.1161408	At5g53090	oxidoreductase, putative
	−1.4119272	At1g76570	chlorophyll A-B binding family protein

Notes. (A) and (B) represent the genes for antioxidant enzymes and photosynthesis, which were selected by the authors by the gene name. Transcript levels were calculated as an average $\log_2$(FC) of the irradiated samples relative to their respective controls. FC, fold change.

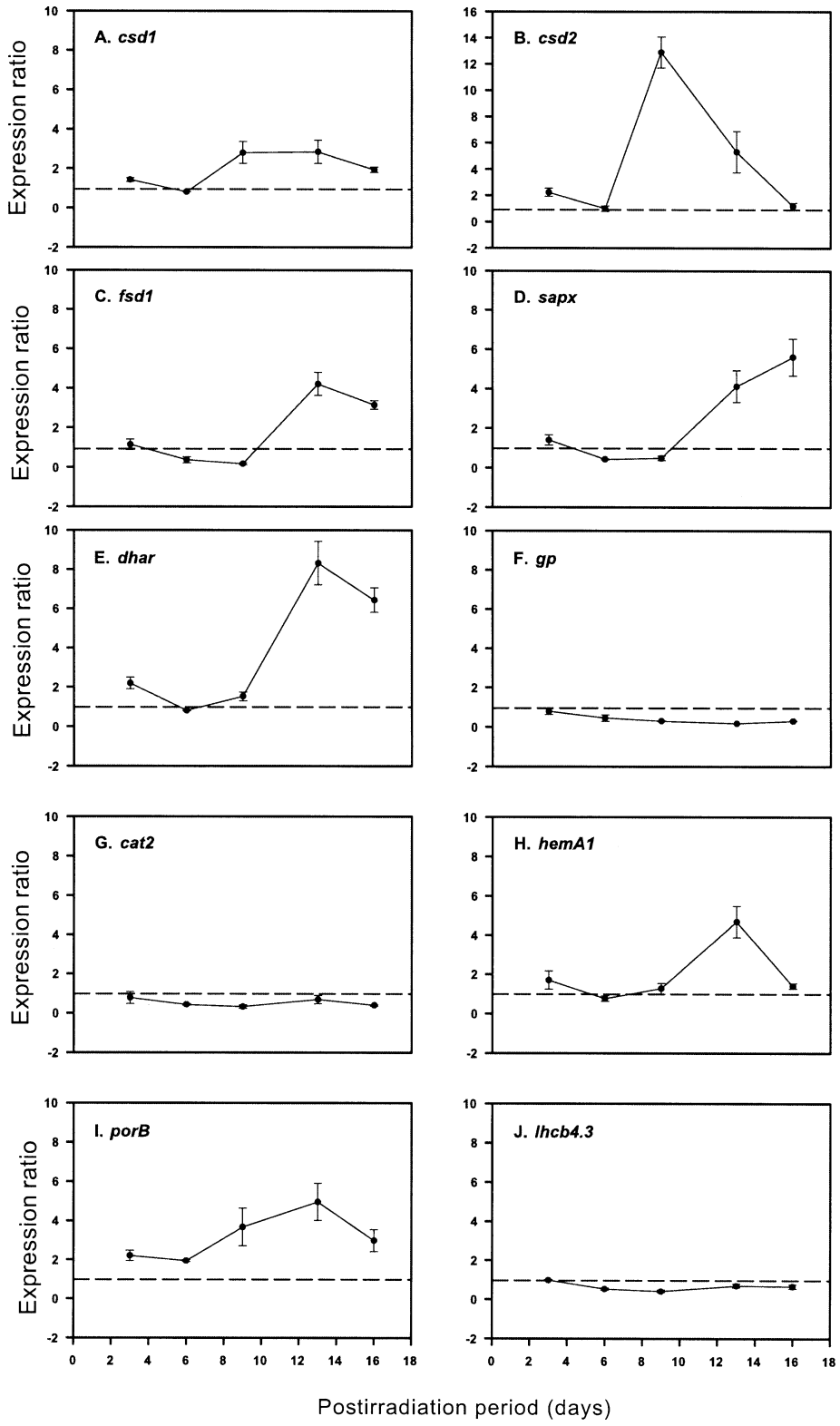

FIG. 5. Real-time quantitative PCR analysis of 10 genes selected from two radiation-responsive categories for validation of the microarray results. Panel A: Cytosolic Cu/Zn-superoxide dismutase (SOD) (*csd1*, At1g08830); panel B: chloroplastic Cu/Zn-SOD (*csd2*, At2g40100); panel C: chloroplastic Fe-SOD (*fsd1*, At4g25100); panel D: stromal ascorbate peroxidase (*sapx*, At4g08390); E, dehydroascorbate reductase (*dhar*, At1g19570); F, glutathione peroxidase (*gp*, At4g31870); G, catalase 2 (*cat2*, At4g35090); H, glutamyl-tRNA reductase 1 (*hemA1*, At1g58290); I, NADPH-protochlorophyllide oxidoreductase B (*porB*, At4g27440); and J, chlorophyll A-B binding protein 4.3 (*lhcb4.3*, At2g40100). Expression ratios were calculated by the comparative ($2^{-\Delta\Delta Ct}$) method. *Actin2* was used as an endogenous control gene to normalize for differences in the amounts of total RNA. Error bars represent means ± SD ($n = 3$).

TABLE 5
Pathway Analysis of the Differentially Expressed Genes during the Postirradiation Period

Differentially expressed genes	No. of genes selected	No. of genes with pathway	KEGG pathway	Gene counts
3	561	6	Pyrimidine metabolism	2
			Cysteine metabolism	1
			Flavonoid biosynthesis	1
			Glutathione metabolism	1
			Methionine metabolism	1
6	1468	22	Stilbene, coumarine and lignin biosynthesis	6
			Ascorbate and aldarate metabolism	4
			Fluorene degradation	4
			Limonene and pinene degradation	4
			Pyrimidine metabolism	4
9	3900	72	Ribosome	24
			Stilbene, coumarine and lignin biosynthesis	12
			Ascorbate and aldarate metabolism	10
			Fluorene degradation	10
			Limonene and pinene degradation	10
13	1785	37	Stilbene, coumarine and lignin biosynthesis	7
			gamma-Hexachlorocyclohexane degradation	6
			Limonene and pinene degradation	6
			Fluorene degradation	6
			Ascorbate and aldarate metabolism	6
16	1090	17	Glycine, serine and threonine metabolism	4
			Pyrimidine metabolism	3
			gamma-Hexachlorocyclohexane degradation	2
			Vitamin B6 metabolism	2
			Stilbene, coumarine and lignin biosynthesis	2

Notes. List includes the top five pathways based on gene counts. Differentially expressed genes of the irradiated samples relative to their respective controls were selected, and then genes with pathway information were used for the analysis.

ters 3 and 6) in the control leaves and three (Clusters 2, 4, and 6) in the irradiated ones (Figs. 2B and 3B).

The 200 differentially expressed genes with the greatest changes from the data used for Fig. 1 were classified into functional subgroups by BINGO, an algorithm for Gene Ontology (GO) significance analysis (*41*) (Table 2). The GO category (GOC) consisted of biological process (BP), cellular component (CC), and molecular function (MF). Genes with stress/stimulus-responsive GO terms were up-regulated in the control leaves, but cell wall/membrane- and development-related genes were down-regulated (Table 2A). This is probably due to the progress of leaf senescence. In contrast, the irradiated leaves showed up-regulation in a defense response-related GO term (Table 2B), which is in good agreement with previous reports of increased gene expression and activities of antioxidant enzymes in irradiated plants (*13, 15, 31*). Together with these results, the reduced expressions of genes with rhythmic process-, circadian rhythm-, and auxin stimulus-related GO terms explain the inhibition in stem growth and retardation in leaf senescence we observed in the irradiated leaves (supplementary Fig. S1). Moreover, the pronounced change in expression of the transcription regulator-related genes may imply that a broad spectrum of genes are affected in irradiated leaves. However, the pathway analysis of the differentially expressed genes demonstrated that the expressions of the photosynthesis-related genes are relatively constant in the irradiated leaves during the reproduction stage (Table 3).

Comparison of Gene Expression in Control and Irradiated Leaves during the Reproduction Stage

To investigate effects of γ radiation on genome-wide gene expression during the reproduction stage, transcript levels of genes in irradiated leaves were compared to those in the respective controls at 3, 6, 9, 13 and 16 days after irradiation. Differentially expressed genes with a twofold change were selected, and a significance level of 0.05 after $\log_2$ transformation of the normalized data was used. As discussed above for Table 2B, radiation caused a significant change in the expression of numerous genes (Fig. 4). The most striking change in gene expression was observed at 9 days after irradiation, when 2164 and 1735 genes were up- and down-regulated, respectively.

ROS are among the most decisive mediators in intracellular signaling of radiation responses. Cellular responses to radiation can occur through direct participation of ROS in cell signaling (*18, 19*) and/or indirect involvement of LMW signaling factors released from the reactions of ROS and

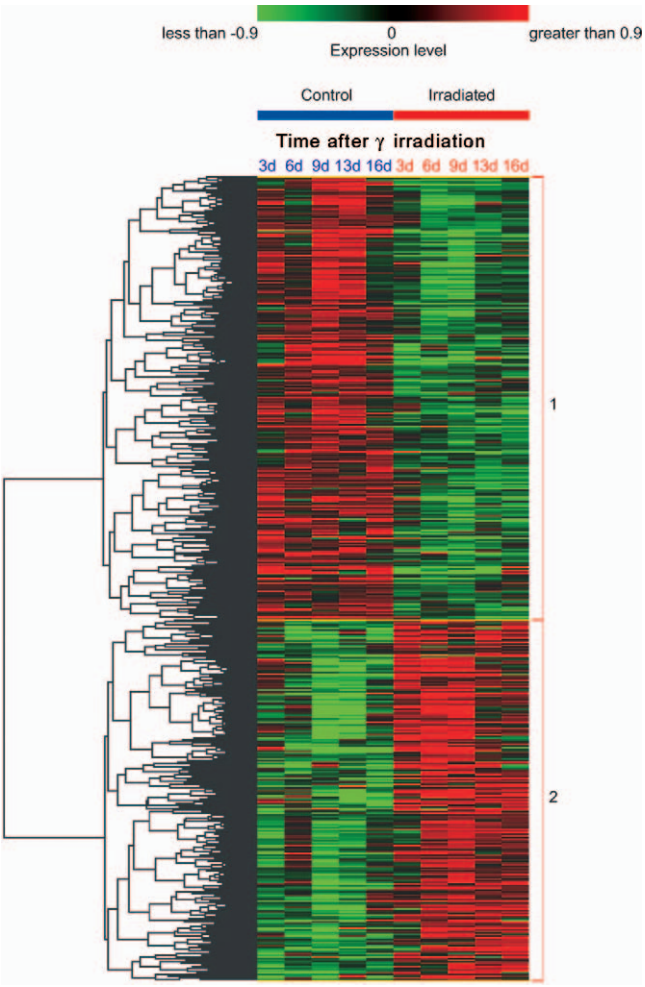

FIG. 6. Hierarchical cluster analysis of 2856 genes with ≤0.05 significance in the Welch's *t* test of the control and irradiated groups. Each horizontal line shows the expression data for one gene after normalization at the times indicated. Colors show the normalized expression levels. Induction (or repression) ranges from black to red (or green) with a fold-change scale bar shown above the cluster. Numbers (1 and 2) indicate defined sub-branches or clusters.

neighboring cellular components (*20, 21*). Therefore, we attempted to analyze the expression of genes for ROS-scavenging antioxidant enzymes as crucial factors in the propagation of radiation responses (Table 4A). Some of them were confirmed by real-time quantitative PCR using the same RNA samples.

Transcription levels of cytosolic Cu/Zn-superoxide dismutase (cytCu/Zn-SOD, *csd1*, accession no. At1g08830), chloroplastic Cu/Zn-SOD (chlCu/Zn-SOD, *csd2*, accession no. At2g40100), and dehydroascorbate reductase (DHAR, *dhar*, accession no. At1g19570) genes were higher overall in the irradiated leaves than in the control ones during the postirradiation period, reaching maximum levels at 9 or 13 days after irradiation (Fig. 5A, B and E). In contrast, the expressions of the glutathione peroxidase (GP, *gp*, accession no. At4g31870) and catalase 2 (CAT2, *cat2*, accession no. At4g35090) genes remained lower in the irradiated leaves during the same period (Fig. 5F and G). Interestingly, the transcript levels of the chloroplastic Fe-SOD (chlFe-SOD, *fsd1*, accession no. At4g25100) and stromal ascorbate peroxidase (sAPX, *sapx*, accession no. At4g08390) genes fluctuated more dramatically, remaining lower in the irradiated leaves until 9 days after irradiation and becoming higher afterward (Fig. 5C and D). Although changes in the expression levels of the genes were not the same in the microarray and real-time PCR results due to the normalization for the former and the comparative expression for the latter using *actin2* as an internal control gene, the overall expression patterns of the genes were similar in the two systems. These data are in good agreement with high SOD and low CAT activities in plants after an acute exposure to relatively high doses of radiation (*15, 48*). However, the distinct expression patterns of antioxidant enzyme genes during the postirradiation period may indicate the existence of a complicated and controlled gene regulation system for radiation-induced gene responses in plants. Similarly, the differential expression patterns for the genes encoding the SOD, APX and CAT isoenzymes have been reported in rice plants after γ irradiation under salt stress (*22*). The results shown in Table 5 suggest that the differentially expressed genes for ascorbate/glutathione metabolism may contribute to the radiation-induced stress and defense signaling (*49*). The high gene count for ribosome at 9 days after irradiation can be correlated with the maximum change in gene expression, as shown in Fig. 4.

Distinctive changes in photosynthesis and pigment metabolism of plants after radiation exposure have been documented (*11, 15, 50, 51*). In particular, a high dose of radiation could cause specific physical alterations in *Arabidopsis* seedlings at certain developmental stages, such as accumulation of chlorophyll and carotenoid and elevation in photosynthetic saturation for light use as well as inhibition of stem growth and retardation of leaf senescence. Although the expressions of the photosynthesis-related genes are relatively constant in the irradiated leaves during the reproduction stage compared to those at 3 days after irradiation (Table 3), their relative expressions compared to the respective controls showed significant radiation-induced changes in photosynthesis and pigment metabolism (Table 4B, Fig. 5H, I and J). Expression of glutamyl-tRNA reductase 1 (HEMA1, *hemA1*, accession no. At1g58290), NADPH-protochlorophyllide oxidoreductase A (PORA, *porA*, accession no. At5g54190), and NADPH-protochlorophyllide oxidoreductase B (PORB, *porB*, accession no. At4g27440) was increased during the postirradiation period, with maximum levels reached at different times. Differential but increased transcript levels of these genes, which encode two major enzymes for chlorophyll synthesis (*52, 53*), may contribute to the increased chlorophyll content of the irradiated leaves at 13 and 16 days after irradiation (supplementary Fig. S1). In contrast, genes of chlorophyll A-B binding proteins 2:4 (LHCB2:4, *lhcb2:4*, accession no. At3g27690) and 4.3 (LHCB4.3, *lhcb4.3*, acces-

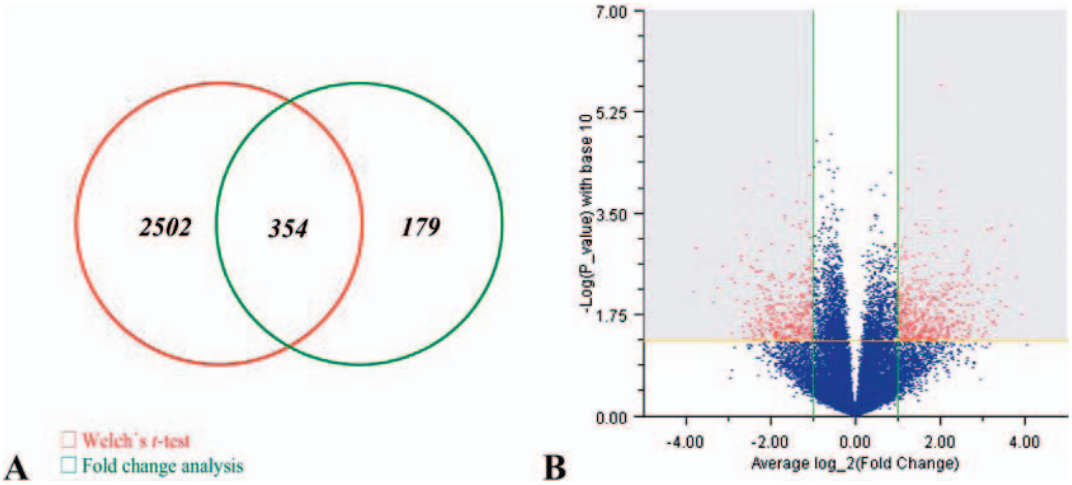

FIG. 7. Distribution of the genes from Welch's *t* test of the control and irradiated groups. Panel A: Filtered data for twofold-change genes (533 genes) and ≤0.05 significance in Welch's *t* test (2856 genes). Panel B: Unfiltered data for comparison of the control and irradiated groups. Red spots represent 354 genes in common of the fold-change analysis and the Welch's *t* test, while blue ones indicate the other 2681 of the total 3035 genes.

sion no. At2g40100) showed opposite expression patterns; the former showed higher transcript levels in the irradiated leaves than in the controls during the postirradiation period while the latter showed the reverse. The alternative expression of *lhcb2:4* can be correlated with retardation of leaf senescence in the irradiated leaves during the reproduction stage (supplementary Fig. S1).

Comparison of Gene Expression in the Control and Irradiated Groups throughout the Reproduction Stage

To compare transcript levels of genes in the control and irradiated groups during the postirradiation period, we carried out clustering analysis of 2856 genes below the 0.05 level of significance in Welch's *t* test (Fig. 6). The genes were divided into two subgroups (Clusters 1 and 2) based on the expression pattern. Expression of Cluster 1 genes (1570 genes) was decreased in the irradiated leaves, while that of Cluster 2 genes (1286 genes) was increased. Furthermore, filtered data for genes with more than a twofold change (533 genes) and changes with less than 0.05 significance in Welch's *t* test (2856 genes) included 354 differentially expressed genes, of which 225 were up-regulated and 129 down-regulated in the irradiated group (Fig. 7). However, only *porB, lhcb4.3, cat2* and *lhcb2:4* among the genes listed in Table 4 were selected in common with the 354 differentially expressed genes (supplementary Table S1). The other genes, especially the antioxidant genes confirmed in Fig. 5, were not selected as significant differentially expressed genes in the comparison of the control and irradiated groups. This can be attributed to the transience and fluctuation of their expressions, which changed throughout the postirradiation period. Instead, the involvement of two ribonucleotide reductase genes (accession nos. At2g21790 and At3g27060), which are critical for cell cycle progression, DNA damage repair, and plant development (*54*), implicated the most well-known genetic response for recovery in the irradiated leaves. This may be involved in the sudden increase of affected genes at 9 days after irradiation (Fig. 4).

In the present study, we showed changes in transcript levels of *csd1, csd1, fsd1, sapx, dhar, cat2* and *gp* in leaves during the 16-day period after γ irradiation of plants at the early reproduction stage. Most of these enzymes belong to ascorbate-glutathione pathway, and they scavenge ROS or its derivatives (*55*). Interestingly, we found low transcript levels of *cat2* and *gp* in the irradiated leaves. Although these results are partly predictable from our previous studies (*15, 22*), there are also opposing results with chronic radiation-induced responses (*13*). Similarly, the expression of *cat2* was strongly induced by UV-light pulses (290 to 400 nm) in leaves of maize seedlings (*56*). Accordingly, the transcription of these genes appears to be inhibited after exposure to an acute dose of radiation. In contrast, the expression patterns of *hemA1, porA, porB, lhcb2:4* and *lhcb4.3* can be correlated with the physiological changes in the irradiated leaves, e.g., retardation in leaf senescence, accumulation of chlorophyll and carotenoid, and elevation of photosynthetic saturation for light use (Table 4 and supplementary Fig. S1). Together with *cat2*, however, *porB* and *lhcb4.3* belong to the most distinguishable genes in terms of the expression change throughout the postirradiation period (data not presented).

Recently, Nagata *et al.* (*31*) reported the results of microarray analysis of genes that respond to ionizing radiation in *Arabidopsis*. Their study focused on the short-term effect of ionizing radiation on the expression of genes within 24 h after γ irradiation with a dose of 3 kGy, which makes the subsequent growth and survival of plants impossible. In contrast, we attempted to determine the long-term effects of ionizing radiation on the genome-wide expression of genes in *Arabidopsis* rosette leaves during the reproductive stage, which is responsible for the phenotypic and physiological changes in the irradiated leaves.

In conclusion, we generated genome-wide transcriptomic profiles of radiation-responsive genes in plants at the reproductive stage using the *Arabidopsis* genome array and revealed the changes in expression of the genes involving in antioxidative defense, photosynthesis and chlorophyll synthesis. Considering the importance of the ROS scavenging system and pigment metabolism in the radiation-induced responses of plants, our results could allow deeper insight into the long-term changes in the functional genes in plants after radiation exposure. Next we are going to use the expression profile to elucidate transcription factors orchestrating the expressions of radiation-responsive genes, especially those related to antioxidative defense and pigment metabolism.

SUPPLEMENTARY INFORMATION

Supplemental document containing additional information about methodology: http://dx.doi.org/10.1667/RR0963.1.s1.

FIG. S1. Phenotypic and physiological differences between the control and irradiated seedlings after γ irradiation: http://dx.doi.org/10.1667/RR0963.1.s2.

TABLE S1. Expression profile of 225 induced and 129 repressed genes in the irradiation groups from the 354 differentially expressed genes selected in Fig. 6: http://dx.doi.org/10.1667/RR0963.1.s3.

ACKNOWLEDGMENT

This project has been carried out under the Nuclear R&D Program by Ministry of Science and Technology, Republic of Korea.

Received: January 16, 2007; accepted: March 28, 2007

REFERENCES

1. H. Goda, S. Sawa, T. Asami, S. Fujioka, Y. Shimada and S. Yoshida, Comprehensive comparison of auxin-regulated and brassinosteroid-regulated genes in *Arabidopsis*. *Plant Physiol.* **134**, 1555–1573 (2004).
2. I. Gadjev, S. Vanderauwera, T. S. Gechev, C. Laloi, I. N. Minkov, V. Shulaev, K. Apel, D. Inzé, R. Mittler and F. V. Breusegem, Transcriptomic footprints disclose specificity of reactive oxygen species signaling in *Arabidopsis*. *Plant Physiol.* **141**, 436–445 (2006).
3. Y. Nakahata, M. Akashi, D. Trcka, A. Yasuda and T. Takumi, The *in vitro* real-time oscillation monitoring system identifies potential entrainment factors for circadian clocks. *BMC Mol. Biol.* **7**, 5 (2006).
4. B. W. Shirley, S. Hanley and H. M. Goodman, Effects of ionizing radiation on a plant genome: Analysis of two Arabidopsis *transparent testa* mutations. *Plant Cell* **4**, 333–347 (1992).
5. A. Rafi, J. J. Weiss and C. M. Wheeler, Effect of γ-radiation of aqueous solutions of DNA's of different base composition. *Biochim. Biophys. Acta* **169**, 230–240 (1968).
6. M. C. R. Symons, Direct and indirect damage to DNA by ionizing radiation. *Radiat. Phys. Chem.* **43**, 403–405 (1994).
7. D. Sy, C. Savoye, M. Begusova, V. Michalik, M. Charlier and M. Spotheim-Maurizot, Sequence-dependent variations of DNA structure modulate radiation-induced strand breakage. *Int. J. Radiat. Biol.* **72**, 147–155 (1997).
8. S. Lim, H. Yoon, S. Ryu, J. Jung, M. Lee and D. Kim, A comparative evaluation of radiation-induced DNA damage using real-time PCR: Influence of base composition. *Radiat. Res.* **165**, 430–437 (2006).
9. V. G. Tusher, R. Tibshirani and G. Chu, Significance analysis of microarrays applied to the ionizing radiation response. *Proc. Natl. Acad. Sci. USA* **98**, 5116–5121 (2001).
10. W. Dewitte and J. A. H. Murray, The plant cell cycle. *Annu. Rev. Plant Biol.* **54**, 235–264 (2003).
11. H. Wada, T. Koshiba, T. Matsui and M. Sato, Involvement of peroxidase in differential sensitivity to γ-radiation in seedlings of two *Nicotiana* species. *Plant Sci.* **132**, 109–119 (1998).
12. T. Nagata, S. Todoriki, T. Hayashi, Y. Shibata, M. Mori, H. Kanegae and S. Kikuchi, γ-Radiation induces leaf trichome formation in *Arabidopsis*. *Plant Physiol.* **120**, 113–119 (1999).
13. R. Zaka, C. M. Vandecasteele and M. T. Misset, Effects of low chronic doses of ionizing radiation on antioxidant enzymes and G_6PDH activities in *Stipa capillata* (Poaceae). *J. Exp. Bot.* **53**, 1979–1987 (2002).
14. M. Kalimullah, J. U. Gaikwad, S. Thomas, A. Sarma and P. B. Vidyasagar, Assessment of ^{1}H heavy ion irradiation induced effects in the development of rice (*Oryza sativa* L.) seedlings. *Plant Sci.* **165**, 447–454 (2003).
15. J-H. Kim, B. Y. Chung, J. S. Kim and S. G. Wi, Effects of in planta gamma-irradiation on growth, photosynthesis, and antioxidative capacity of red pepper (*Capsicum annuum* L.) plants. *J. Plant Biol.* **48**, 47–56 (2005).
16. J. F. Ward, Radiolytic damage to genetic material. *J. Chem. Edu.* **58**, 135–139 (1981).
17. C. von. Sonntag, *The Chemical Basis of Radiation Biology.* Taylor & Francis, New York, 1987.
18. T. D. Luckey, *Hormesis with Ionizing Radiation.* CRC Press, Boca Raton, FL, 1980.
19. M. W. Miller, Radiation hormesis in plants. *Health Phys.* **52**, 607–616 (1987).
20. T. D. Luckey, *Radiation Hormesis.* CRC Press, Boca Raton, FL, 1991.
21. L. Eidus, Hypothesis regarding a membrane-associated mechanism of biological action due to low-dose ionizing radiation. *Radiat. Environ. Biophys.* **39**, 189–195 (2000).
22. J-H. Kim, B. Y. Chung, M-H. Baek, S. G. Wi, D-H. Yang, M. C. Lee and J-S. Kim, Expression of antioxidant isoenzyme genes in rice under salt stress and effects of jasmonic acid and γ-radiation. *Agric. Chem. Biotechnol.* **48**, 1–6 (2005).
23. K. M. Ramonell, B. Zhang, R. M. Ewing, Y. Chen, D. Xu, G. Stacey and S. Somerville, Microarray analysis of chitin elicitation in *Arabidopsis thaliana*. *Mol. Plant Pathol.* **3**, 301–311 (2002).
24. F. Liu, T. Vantoai, L. P. Moy, G. Bock, L. D. Linford and J. Quackenbush, Global transcription profiling reveals comprehensive insights into hypoxic response in *Arabidopsis*. *Plant Physiol.* **137**, 1115–1129 (2005).
25. M. Menges, L. Henning, W. Gruissem and J. A. H. Murray, Cell cycle-regulated gene expression in *Arabidopsis*. *J. Biol. Chem.* **277**, 41987–42002 (2002).
26. M. Menges, L. Henning, W. Gruissem and J. A. H. Murray, Genome-wide gene expression in an *Arabidopsis* cell suspension. *Plant Mol. Biol.* **53**, 423–442 (2003).
27. P. Costaglioli, J. Joubès, C. Garcia, M. Stef, B. Arveiler, R. Lessire and B. Garbay, Profiling candidate genes involved in wax biosynthesis in *Arabidopsis thaliana* by microarray analysis. *Biochim. Biophys. Acta* **1734**, 247–258 (2005).
28. K. M. Culligan, C. E. Robertson, J. Foreman, P. Doerner and A. B. Britt, ATR and ATM play both distinct and additive roles in response to ionizing radiation. *Plant J.* **48**, 947–961 (2006).
29. H. S. Cho, H. S. Lee and H-S. Pai, Expression patterns of diverse genes in response to gamma irradiation in *Nicotiana tabacum*. *J. Plant Biol.* **43**, 82–87 (2000).
30. T. Nagata, H. Yamada, Z. Du, S. Todoriki and S. Kikuchi, Microarray analysis of genes that respond to γ-irradiation in *Arabidopsis*. *J. Agric. Food Chem.* **53**, 1022–1030 (2005).
31. T. Sahr, G. Voigt, W. Schimmack, H. G. Paretzke and D. Ernst, Low-

level radiocaesium exposure alters gene expression in roots of *Arabidopsis*. *New Phytol.* **168**, 141–148 (2005).

32. J. G. Berrin, O. Pierrugues, C. Brutesco, B. Alonso, J. L. Montillet, D. Roby and M. Kazmaier, Stress induces the expression of *AtNADK-1*, a gene encoding a NAD(H) kinase in Arabidopsis thaliana. *Mol. Genet. Genomics* **273**, 10–9 (2005).

33. O. Pierrugues, C. Brutesco, J. Oshiro, M. Gouy, Y. Deveaux, G. M. Carman, P. Thuriaux and M. Kazmaier, Lipid phosphate phosphatases in Arabidopsis. Regulation of the *AtLPP1* gene in response to stress. *J. Biol. Chem.* **276**, 20300–20308 (2001).

34. G. Doucet-Chabeaud, C. Godon, C. Brutesco, G. de Murcia and M. Kazmaier, Ionising radiation induces the expression of PARP-1 and PARP-2 genes in *Arabidopsis*. *Mol. Genet. Genomics* **265**, 954–963 (2001).

35. Y. Deveaux, B. Alonso, O. Pierrugues, C. Godon and M. Kazmaier, Molecular cloning and developmental expression of *AtGR1*, a new growth-related Arabidopsis gene strongly induced by ionizing radiation. *Radiat. Res.* **154**, 355–364 (2000).

36. D. Abarca, M. Martin and B. Sabater, Differential leaf stress responses in young and senescent plants. *Physiol. Plant.* **113**, 409–415 (2001).

37. A. R. Rabas and C. E. Martin, Movement of water from old to young leaves in three species of succulents. *Ann. Bot.* **92**, 529–536 (2003).

38. M. Eisen, P. T. Spellman, P. O. Brown and D. Botstein, Cluster analysis and display of genome-wide expression patterns. *Proc. Natl. Acad. Sci. USA* **95**, 14863–14868 (1998).

39. T. R. Golub, D. K. Slonim, P. Tamayo, C. Huard, M. Gaasenbeek, J. P. Mesirov, H. Coller, M. L. Loh, J. R. Downing and E. S. Lander, Molecular classification of cancer: Class discovery and class prediction by gene expression monitoring. *Science* **286**, 531–537 (1999).

40. S. Seno, R. Teramoto, Y. Takenaka and H. Matsuda, A method for clustering gene expression data based on graph structure. *Genome Informatics* **15**, 151–160 (2004).

41. S. G. Lee, J. S. Yang, W. S. Lee, M. Shin and Y. S. Kim, Extraction of biological contexts and ontological DAG structures from gene groups using GO term distribution. *Genome Informatics* **14**, 683–684 (2003).

42. T. D. Schmittgen, B. A. Zakrajsek, A. G. Mills, V. Gorn, M. J. Singer and M. W. Reed, Quantitative reverse transcription-polymerase chain reaction to study mRNA decay: Comparison of endpoint and real-time methods. *Anal. Biochem.* **285**, 194–204 (2000).

43. M. B. Grace, C. B. McLeland and W. F. Blakely, Real-time quantitative RT-PCR assay of *GADD45* gene expression changes as a biomarker for radiation biodosimetry. *Int. J. Radiat. Biol.* **78**, 1011–1021 (2002).

44. J. Winer, C. K. S. Jung, I. Shackel and P. M. Williams, Development and validation of real-time quantitative reverse transcriptase-polymerase chain reaction for monitoring gene expression in cardiac myocytes *in vitro*. *Anal. Biochem.* **270**, 41–49 (1999).

45. J. C. Game, G. W. Birrell, J. A. Brown, T. Shibata, C. Baccari, A. M. Chu, M. S. Williamson and J. M. Brown, Use of a genome-wide approach to identify new genes that control resistance of *Saccharomyces cerevisiae* to ionizing radiation. *Radiat. Res.* **160**, 14–24 (2003).

46. A. S. Mahmoud-Ahmed, S. Atkinson and C. S. Wong, Early gene expression profile in mouse brain after exposure to ionizing radiation. *Radiat. Res.* **165**, 142–154 (2006).

47. K. Otsuka, T. Koana, H. Tauchi and K. Sakai, Activation of antioxidant enzymes induced by low-dose-rate whole-body γ irradiation: Adaptive response in terms of initial DNA damage. *Radiat. Res.* **166**, 474–478 (2006).

48. H. S. Lee, S. H. You, S. Y. Kwon, J-S. Kim and S-S. Kwak, Gamma radiation-induced changes of antioxidant enzymes in callus cultures of cassava (*Manihot esculenta* Crantz). *Kor. J. Plant Tiss. Cult.* **26**, 53–58 (1999).

49. G. Noctor and G. H. Foyer, Ascorbate and glutathione: Keeping active oxygen under control. *Annu. Rev. Plant Physiol. Plant Mol. Biol.* **49**, 249–279 (1998).

50. L. Frylink, I. A. Dubery and J. C. Schabort, Biochemical changes involved in stress response and ripening behavior of gamma-irradiated mango fruit. *Phytochemistry* **26**, 681–686 (1987).

51. J-H. Kim, M-H. Baek, B. Y. Chung, S. G. Wi and J-S. Kim, Alterations in the photosynthetic pigments and antioxidant machineries of red pepper (*Capsicum annuum* L.) seedlings from gamma-irradiated seeds. *J. Plant Biol.* **47**, 314–321 (2004).

52. S. I. Beale, Enzymes of chlorophyll biosynthesis. *Photosynth. Res.* **60**, 43–73 (1999).

53. U. Eckhardt, B. Grimm and S. Hörtensteiner, Recent advances in chlorophyll biosynthesis and breakdown in higher plants. *Plant Mol. Biol.* **56**, 1–14 (2004).

54. C. Wang and Z. Liu, Arabidopsis ribonucleotide reductases are critical for cell cycle progression, DNA damage repair, and plant development. *Plant Cell* **18**, 350–365 (2006).

55. K. Asada, The water-water cycle in chloroplasts: Scavenging of active oxygens and dissipation of excess photons. *Annu. Rev. Plant Physiol. Plant. Mol. Biol.* **50**, 601–639 (1999).

56. R. Boldt and J. G. Scandalios, Influence of UV-light on the expression of the Cat2 and Cat3 catalase genes in maize. *Free Radic. Biol. Med.* **23**, 505–514 (1997).